JACS
JOURNAL OF THE AMERICAN CHEMICAL SOCIETY

COMMUNICATION

pubs.acs.org/JACS

Gap Distance and Interactions in a Molecular Tunnel Junction

Shuai Chang,[†] Jin He,[‡] Peiming Zhang,[‡] Brett Gyarfas,[†] and Stuart Lindsay*[,†,‡,§]

[†]Department of Physics, [‡]Biodesign Institute, and [§]Department of Chemistry and Biochemistry, Arizona State University, Tempe, Arizona 85287, United States

Supporting Information

ABSTRACT: The distance between electrodes in a tunnel junction cannot be determined from the external movement applied to the electrodes because of interfacial forces that distort the electrode geometry at the nanoscale. These distortions become particularly complex when molecules are present in the junction, as demonstrated here by measurements of the AC response of a molecular junction over a range of conductivities from microsiemens to picosiemens. Specific chemical interactions within the junction lead to distinct features in break-junction data, and these have been used to determine the electrode separation in a junction functionalized with 4(5)-(2-mercaptoethyl)-1*H*-imidazole-2-carboxamide, a reagent developed for reading DNA sequences.

Adjustable tunnel junctions are widely used to determine the electrical properties of molecules spanning two electrodes.[1] The size of the junction is usually characterized by the measured tunnel conductance of the junction or by the amount by which a break junction is separated by an externally applied displacement. The actual size of the nanoscale gap is not readily determined from the external measurement. When the electrodes (usually gold) are metallically bonded and then pulled apart to form a break junction, plastic deformation of the gold leads to the formation of filaments that give rise to a constant conductance over distances that approach a nanometer (see Figure 3A for an example). When the filaments break, the metal surface relaxes back to a more stable configuration (i.e., they "snap back"). On approach of two metal surfaces, the electrodes can be drawn together by van der Waals interactions when they are close together, leading to instabilities in the gap. The electrodes can be repelled as contamination is trapped in the gap, leading to apparent approach distances of 100 nm or more. Examples of these events are given in Figures S1 and S2 in the Supporting Information (SI). It is important to be able to determine the actual value of the nanoscale gap when the goal of these studies is to make devices that utilize fixed, nanofabricated tunnel junctions.

We have proposed a readout system for DNA sequences based on a noncovalent complex between recognition molecules tethered to fixed electrodes and the bases of a DNA molecule that is passed through the tunnel junction by electrophoresis.[2] Here we report on a study of tunnel junctions based on gold electrodes functionalized with a new generation of recognition molecule, 4(5)-(2-mercaptoethyl)-1*H*-imidazole-2-carboxamide (hereafter called imidazole-2-carboxamide; Figure 1B). The synthesis and characterization of this molecule has been described elsewhere.[3] We used ac modulation of the gap[4] as a probe of the effective stiffness of the gap, employing a logarithmic current-to-voltage converter to probe a range of gap conductances from close to quantum point contact (conductance = $G_0 = 2e^2/h = 77\ \mu$S) all the way out to the small conductances used to pass DNA bases between the electrodes ($\sim$ 6 pS). These measurements revealed the many interactions taking place in the tunnel junction, interactions that make it impossible to determine the gap from tunnel-current data alone. We determined the gap size using molecules trapped in the gap as a "molecular ruler", with the molecular tunneling signals ceasing when the gap size exceeded the size of the trapped molecules.[5] The gap size determined in this way was $\sim$24 Å, which is more than large enough to pass a single-stranded DNA molecule.

Monolayers of imidazole-2-carboxamide were formed on freshly flame-annealed Au(111) electrodes and characterized with FTIR spectroscopy, ellipsometry, X-ray photoelectron spectroscopy (XPS) and scanning tunneling microscopy (STM) (Figures S3−S5). Importantly, ellisometry and XPS taken together suggest that the molecules stand upright on the surface with the S bonded to gold, forming a film consistent with the full 8.5 Å length of the recognition molecules. STM probes were etched from gold wire, insulated with high-density polyethylene, and functionalized as described previously (see ref 2 and the SI). The functionalization of the probes was tested by comparing tunneling signals obtained on bare substrates with tunneling signals obtained from bare (i.e., unfunctionalized) probes on functionalized substrates. Tunneling measurements were recorded with an Agilent PicoSPM (Chandler, AZ) interfaced to a digital storage oscilloscope and a field-programmable gate array controller (PCIe-7842R, National Instruments). The entire junction was submerged in the 1 mM phosphate-buffered aqueous electrolyte (pH 7) used for readout of DNA sequences.

The modulated-junction method is illustrated in Figure 1. A small distance modulation, A_0, is applied to the gap by adding an ac signal to the voltage used to drive the piezoelectric transducer (PZT) in the vertical direction. The PZT sensitivity was calibrated by using STM images of single-atom steps on Au(111), and an amplitude of $A_0 = 0.52$ Å was used in the present work. This is small enough that the following expression holds for the AC modulation of the gap conductance: $G_{AC} = \beta A_0^{GAP} G_{DC}$, where G_{DC} is the average conductance (see the SI) and A_0^{GAP} is the height modulation of the gap. Thus, the AC signal increases in direct proportion to the DC value, as illustrated with traces of the tunneling signal in Figure 1C. The ratio G_{AC}/G_{DC} (Figure 1D) yields the quantity βA_0^{GAP}. The whole problem lies in the fact that A_0^{GAP} is not equal to the applied modulation A_0 because of the small compliance of the STM probe.[6] Mechanical interactions in

Received: July 20, 2011
Published: August 12, 2011

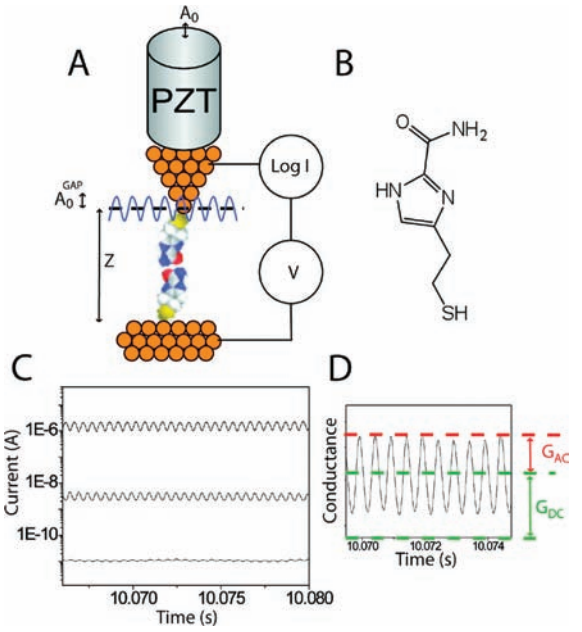

Figure 1. Setup for determining junction stiffness. (A) An ac modulation applied to the PZT deflects it by an amount A_0. The modulation amplitude of the gap itself, A_0^{GAP}, is different because of interaction forces in the tunnel junction. (B) Structure of imidazole-2-carboxamide. (C) AC modulation of the PZT results in a corresponding modulation of the gap conductance that increases with the DC set-point current according to $G_{AC} = \beta A_0^{GAP} G_{DC}$. (D) Illustration showing how the quantities G_{AC} and G_{DC} are extracted.

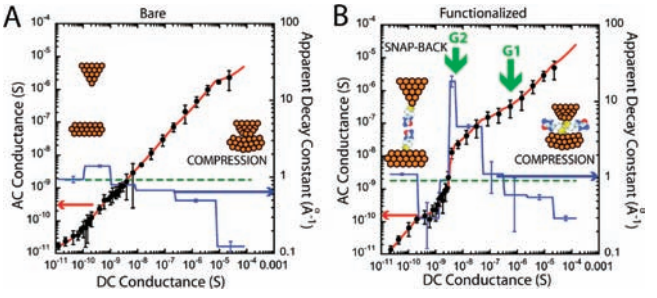

Figure 2. Variation of G_{AC} with G_{DC} for (A) a bare gold probe and bare gold surface in 1 mM phosphate buffer (pH 7.0) and (B) a probe and surface both functionalized with imidazole-2-carboxamide in the same buffer (black dots). The red lines are linear fits to segments of the plots using the effective decay constants (i.e., the apparent β values), as shown by the blue lines (righthand axes of the plots). Rapid changes at the points labeled G1 and G2 are coincident with peaks in the conductance distributions measured by break-junction methods.

the junction show up as rapid variations in the value of "β" derived by assuming a constant A_0. In this work, signals were acquired using a logarithmic current-to-voltage converter[7] that was calibrated as described in the SI.

Figure 2A shows how G_{AC} varies with G_{DC} for a bare gold probe and a bare gold substrate in 1 mM phosphate buffer (pH 7). These data show the mean (data points) and standard deviation for 39 recordings at each G_{DC}, spanning a range from ~20 μS to 10 pS (at a probe bias of +0.5 V). The data were fitted with six linear segments, yielding the values of the apparent decay constant β_{app}, given by $\beta_{app} = (1/A_0)(\partial G_{AC}/\partial G_{DC})$. They recapitulate the

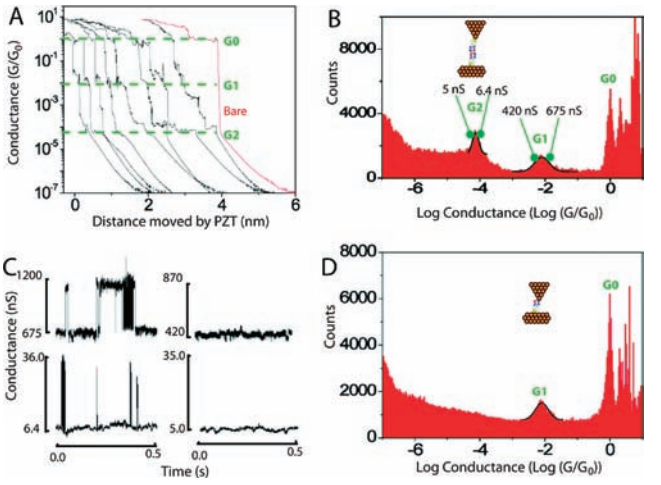

Figure 3. Break-junction measurements of imidazole-2-carboxamide-functionalized tunnel junctions. (A) Typical current−time plots (converted to apparent gap size using the PZT velocity). Distinct plateaus occur near G0 as a result of the formation of quantum point contacts. Features near G1 and G2 are associated with molecular structures formed in the gap. The red curve is typical of data collected for unfunctionalized probes and surfaces. No plateaus are seen below G0. (B) Distribution of conductances when both the probe and surface are functionalized. The lower conductance peak (G2) is not present when only the surface is functionalized (D), showing that this peak is associated with pairs of molecules spanning the gap, an interpretation quantitatively consistent with the values of G1 and G2. (C) Telegraph noise due to stochastic bonding of single molecules across the gap (upper left) or pairs of molecules in series (lower left). The noise vanishes when the gap conductance is adjusted to just below G1 or G2 (traces on the right).

data first reported for aqueous electrolyte by Vaught et al.,[8] who made measurements using a perchlorate electrolyte, whereas we used 1 mM phosphate buffer. Evidently, these ions do not play a significant role. At small gap conductances, β_{app} is ~0.9 Å^{-1}, and it decreases as the gap conductance rises above 10^{-8} S. The decrease is particularly marked above 10^{-5} S, where β_{app} falls to almost 0.1 Å^{-1}, a consequence of strong mechanical interactions in the gap (see the SI). In the absence of such interactions, the gap could be estimated from the sum of the distances z_{nm} corresponding to the linear segments of constant β_{nm} [i.e., $z = -\Sigma(1/\beta_{nm}) \ln(G_m/G_n)$, where G_n is the conductance at the high side of the linear segment and G_m is the conductance on the low side]. Evaluating this sum yields z = 38 Å, a gap that is unrealistically large because it has been exaggerated by the very small value of β_{app} at the highest conductance.

When both electrodes are functionalized with imidazole-2-carboxamide (Figure 2B) the shape of the curve changes dramatically. There is a "bump" for G_{DC} between 10^{-7} and 10^{-9} S where β_{app} reaches the extraordinary value of 18.4 Å^{-1}. Interestingly, β_{app} is not as much reduced at small gaps in comparison with the unfunctionalized system, possibly reflecting a reduced gold−gold interaction. The very large values of β_{app} are most readily explained by regions in which bonds between the probe and surface break, resulting in a snapping back of the electrode surfaces and a large change in current for a small motion of the probe. Jumps in the slope of this plot at ~10^{-7} and 10^{-9} S are associated with molecular adhesion events, as confirmed by break-junction data.[1a] Figure 3A shows some typical curves of current versus retraction distance when both the probe and surface are

functionalized. Plateaus are evident at $\sim 10^{-7}$ S (i.e., $\sim 10^{-2} G_0$, labeled G1) and $\sim 10^{-9}$ S (i.e., $\sim 10^{-4} G_0$, labeled G2). Curves taken with a bare probe (example in red) show only the plateaus near the quantum of conductance (G_0). A histogram of the current recorded from 1000 such curves (Figure 3B) shows distinct peaks at $(6.2 \pm 2.3) \times 10^{-7}$ S [i.e., $\sim 10^{-2} G_0$ (G1)] and $(5.8 \pm 0.7) \times 10^{-9}$ S [i.e., $\sim 10^{-4} G_0$ (G2)]. The likely origin of the two peaks is immediately clear when similar curves are collected and histogrammed using a bare tip and a functionalized surface (Figure 3D). In this case, only peak G1 appears in addition to the metallic contact peak at G_0. Thus, the high-current peak (at G1) is assigned to one molecule spanning the gap (via an amine−gold linkage[9]), while the low-current peak (G2) is assigned to hydrogen-bonded pairs bridging the gap. Time traces of the tunnel-current noise taken at conductances above G1 and G2 (Figure 3C) show the characteristic "telegraph" noise fluctuations due to stochastic bond breaking in a molecule spanning the junction.[5] No signals are seen when the set point is below G1 or G2 (it should be noted that signals due to hydrogen-bonded pairs of molecules spanning the gap are too small to be seen in the traces collected near G1).

Is this assignment of G1 to one molecule and G2 to a pair in series consistent with the observation that $\beta \approx 0.5-0.6$ when the molecules are interacting (Figure 2B)? Using $\beta = -\ln(G_{1,2}/G_0)/z_{1,2}$ with G1 = 621 nS (Figure 3B) and z_1= 8.5 Å gives β = 0.57 $Å^{-1}$, while using G2 = 5.8 nS (Figure 3B) and z_2 = 17 Å gives β = 0.58 $Å^{-1}$, consistent with one molecular length trapped in the gap at G1 and two molecular lengths trapped in the gap at G2.

The magnitude of the telegraph noise measures how much the conductance increases when molecules bond the two electrodes together. For the single molecule, the conductance increase upon bonding is 432 nS, while for the two molecules in series, this value is 28 nS (see the SI). On the basis of distance differences alone, assuming that β is still 0.6 $Å^{-1}$ leads to an estimate of $\exp(-\beta L + 2\beta L) = \exp(\beta L)$ =164:1 for the ratio of the two conductances. This is much larger than the observed ratio (15:1), showing that details of the bonding play a large role in determining the size of the telegraph noise. It should be noted that events that cause "electronic bond fluctuations" of the electrodes are not the same as the formation and breaking of the chemical bonds between the molecules and electrodes, as discussed in detail elsewhere.[2]

We are still left with the question of what the final gap is at the 6 pS conductance (G_{SP}) used for identifying DNA bases. Given that the gap at G2 is 17 Å and taking the actual value of β in water to be 0.92 [Figure 2A; it appears to be less just after the bonds break in the case of the functionalized junction (Figure 2B) because of attraction between the bonding groups], we estimate the additional distance from G1 to G_{SP} to be 7.5 Å, for a total gap size of ∼24 Å.

In summary, we have shown how the formation of molecular complexes in a tunnel junction is signaled by changes in the elastic properties of the tunnel junction (which are evident in the ac response of the junction) and how the structures themselves can be used as nanoscale "rulers" to determine the size of the nanojunction.

■ ASSOCIATED CONTENT

Ⓢ Supporting Information. DC adjustment of the gap and mechanical interactions, preparation and characterization of monolayers of imidazole-2-carboxamide on Au(111), preparation and functionalization of STM probes, large- and small-amplitude expressions for G_{AC}, calibration of the logarithmic amplifier, and telegraph noise data for the conductance of single molecules. This material is available free of charge via the Internet at http://pubs.acs.org.

■ AUTHOR INFORMATION

Corresponding Author
stuart.lindsay@asu.edu

■ ACKNOWLEDGMENT

This work was supported by the National Human Genome Research Institute under Grants R21 HG005851 and R21 HG004378. We thank Dr. Shengqing Li for the ellipsometry, FTIR, and XPS analyses and Dr. Feng Liang for synthesis of reagents.

■ REFERENCES

(1) (a) Xu, B.; Tao, N. J. *Science* **2003**, *301*, 1221–1223. (b) Venkataraman, L.; Klare, J. E.; Nuckolls, C.; Hybertsen, M. S.; Steigerwald, M. L. *Nature* **2006**, *442*, 905–907. (c) Lindsay, S.; He, J.; Sankey, O.; Hapala, P.; Jelinek, P.; Zhang, P.; Chang, S.; Huang, S. *Nanotechnology* **2010**, *21*, No. 262001. (d) Tsutsui, M.; Taniguchi, M.; Yokota, K.; Kawai, T. *Nat. Nanotechnol.* **2010**, *5*, 286–290.

(2) Huang, S.; He, J.; Chang, S.; Zhang, P.; Liang, F.; Li, S.; Tuchband, M.; Fuhrman, A.; Ros, R.; Lindsay, S. M. *Nat. Nanotechnol.* **2010**, *5*, 868–873.

(3) Liang, F.; Li, S.; Lindsay, S.; Zhang, P. *Chemistry*, submitted.

(4) (a) Xu, B. *Small* **2007**, *3*, 2061–2065. (b) Xia, J. L.; Diez-Perez, I.; Tao, N. J. *Nano Lett.* **2008**, *8*, 1960–1964. (c) Zhou, J.; Chen, G.; Xu, B. *J. Phys. Chem. C* **2010**, *114*, 8587–8592.

(5) (a) Haiss, W.; Wang, C.; Grace, I.; Batsanov, A. S.; Schiffrin, D. J.; Higgins, S. J.; Bryce, M. R.; Lambert, C. J.; Nichols, R. J. *Nat. Mater.* **2006**, *5*, 995–1002. (b) Haiss, W.; Wang, C.; Jitchati, R.; Grace, I.; Martín, S.; Batsanov, A. S.; Higgins, S. J.; Bryce, M. R.; Lambert, C. J.; Jensen, P. S.; Nichols, R. J. *J. Phys: Condens. Matter* **2008**, *20*, No. 374119.

(6) Chang, S.; He, J.; Kibel, A.; Lee, M.; Sankey, O. F.; Zhang, P.; Lindsay, S. M. *Nat. Nanotechnol.* **2009**, *4*, 297–301.

(7) He, J.; Sankey, O. F.; Lee, M.; Tao, N. J.; Li, X.; Lindsay, S. M. *Faraday Discuss.* **2006**, *131*, 145–154.

(8) Vaught, A.; Jing, T. W.; Lindsay, S. M. *Chem. Phys. Lett.* **1995**, *236*, 306–310.

(9) Quek, S. Y.; Neaton, J. B.; Hybertsen, M. S.; Venkataraman, L.; Choi, C. H.; Louie, S. G. *Nano Lett.* **2007**, *7*, 3477–3482.